Tampere University

Matias Mustonen

MAXWELL'S DEMON IN QUANTUM MECHANICS

Simulation of a quantum wave packet in a two-dimensional double cavity system

Engineering and Natural Sciences
Bachelor of Science Thesis
May 2020

ABSTRACT

Matias Mustonen: Maxwell's Demon in Quantum Mechanics
Bachelor of Science Thesis
Tampere University
Science and Engineering
May 2020

Maxwell's demon is a thought experiment in which the second rule of thermodynamics is violated. Originally, the thought experiment consisted of two connected cavities with a filter between them. The demon could choose to let particles go through the connection gap. If the demon were to let faster moving particles to one cavity and slower moving particles to the other cavity it would introduce a temperature difference in the system. Thus, decreasing the total entropy of the system violating the second rule of thermodynamics.

In classical mechanics the experiment can be implemented as a two-dimensional two-cavity system, where one cavity is integrable and the other is chaotic. The probability for a particle to travel from the chaotic cavity to the integrable is greater than vice versa. This creates an imbalance in an observable such as pressure.

In this thesis we investigate the quantum mechanical counterpart of the classical double cavity with one cavity being an integrable rectangle and the other one a chaotic stadium. We initialize the system with a quantum mechanical wave packet in one of the cavities and compute the system's time-evolution. The time-evolution is analyzed with visualizations of the probability density and by inspecting observables related to the system's ergodic properties such as autocorrelation, inverse participation ratio, and information entropy.

If initialized in the chaotic cavity, we have found that the wave packet propagates much faster to the other cavity than if it was initially in the regular cavity. This is a quantum mechanical demonstration of the original Maxwell's thought experiment.

Keywords: Maxwell's demon, quantum billiards, classical billiards

TIIVISTELMÄ

Matias Mustonen: Maxwellin demoni kvanttimekaniikassa
Kandidaatintyö
Tampereen yliopisto
Tekniikan ja luonnontieteet, TkK
Toukokuu 2020

Maxwellin demoni on ajatuskoe, jossa termodynamiikan toinen pääsääntö näennäisesti rikkoontuu. Alun perin ajatuskoe koostui kahdesta kammiosta, jotka on erotettu toisistaan kalvolla. Kalvossa on pieni aukko, jonka läpi hiukkaset voivat siirtyä kammiosta toiseen. Demoni saattaa päästää hiukkasia kalvossa olevan aukon läpi. Jos demoni päästää nopeasti liikkuvia hiukkasia yhteen kammioon ja hitaasti liikkuvia hiukkasia toiseen, muodostuu kammioiden välille lämpötilaero. Näin ajatuskokeessa kokonaisentropia penenisi termodynamiikan toisen pääsäännön vastaisesti.

Ajatuskoe voidaan klassisesti toteuttaa kaksiulotteisena kaksoiskammiosysteeminä, jossa yksi kammio on kaoottinen ja toinen säännöllinen. Hiukkasen todennäkösyys matkustaa kaoottisesta kammiosta toiseen on suurempi kuin päinvastoin. Tästä muodostuu epätasapaino havaittavassa suureessa kuten paineessa, mikä aiheuttaa potentiaalieron kammioiden välille.

Tässä työssä tutkittiin kvanttimekaanista vastinetta klassiselle kaksoiskammiolle, jossa yksi kammio on suorakulmio ja toinen on stadioni. Suorakulmio on säännöllinen kammio ja stadioni kaoottinen. Systeemi alustettiin kvanttimekaanisella aaltopaketilla yhdestä kammiosta ja laskettiin systeemin aikaevoluutiota. Aikaevoluutiota analysoitiin todennäköisyystiheyden visualisoinnin avulla ja tutkimalla havaittavia suureita systeemin ergodisistä ominaisuuksista kuten autokorrelaatiota ja informaatioentropiaa.

Aaltopaketin evoluution alkaessa kaoottisesta kammiosta huomataan, että se siirtyy nopeammin toiseen kammioon kuin toiseen suuntaan. Tämä on kvanttimekaaninen demonstraatio alkuperäisestä Maxwellin ajatuskokeesta.

Avainsanat: Maxwellin demoni, kvanttibiljardi, klassinen biljardi

CONTENTS

1 INTRODUCTION

Maxwell's demon is a phenomenon in physics that seemingly breaks the second law of thermodynamics by forming a potential difference from nothing [1]. More precisely, it describes a tendency to naturally form and sustain a difference for a state variable such as pressure due to varying chaotic dynamics of connected cavities. Chaos is the undeterministic nature of the output in a deterministic system, or simply, the sensitivity of the outcome to the initial conditions.

Classically, such systems are described using classical billiards. In billiard systems particles collide elastically with the cavity boundary [2]. In physics, billiard systems are widely studied in the field of nonlinear dynamics and chaos.

In quantum mechanics there are efforts seeking the relationship of quantum mechanics and classical chaos [3]. Such a field is called quantum chaos. Quantum chaos examines whether quantum mechanics brings forth chaos in the classical limit, which should happen according to the correspondence principle.

In this thesis we study a quantum mechanical wave packet in a double cavity system where one cavity is chaotic and the other integrable, i.e., non-chaotic. By computing the particle probabilities for each cavity, localization measures, and autocorrelation, we demonstrate the emergence of a Maxwell's demon in a quantum mechanical setup.

This thesis is organized as follows. In Ch. 2 we present the theoretical background of the simulation. We review the origin of Maxwell's thought experiment as well as a modern interpretation of it, followed by a brief introduction to classical and quantum billiards. Numerical methods used in this thesis are described in Ch. 3. Finally, in Ch. 4 the calculations based on the simulations is discussed and we determine the existence of Maxwell's demon in a quantum mechanical double cavity.

2 THEORY

2.1 Maxwell's demon

Originally Maxwell described a system of two vessels which contain elastic molecules divided by a diaphragm [4]. Elastic molecules do not lose energy or momentum in collisions [5]. Initially, the vessels have an equal number of particles. The diaphragm has a hole in it through which particles can go from one vessel to another without doing work. Let us suppose that in this system there is a finite being (demon) that knows the locations and velocities of every particle and can open and close the hole in the diaphragm. The demon could let fast-moving particles to one vessel and slow-moving particles to another vessel, while keeping the number of particles equal in the vessels. Thus, the demon could extract energy from a colder vessel to a hotter vessel. This lowers the entropy of the system, which is forbidden by the second law of thermodynamics. However, this seemingly lowered entropy can be corrected with informational entropy which states that the demon raises entropy when storing the needed information to control the system [6, 7].

A modern interpretation of this experiment would be a double cavity system with a semipermeable membrane that lets slow particles in one direction and fast particles to the other direction. This creates a difference in heat and thus a potential difference in the system [1].

2.2 Classical billiards

Classical billiards is a system that has a cavity Q where particles move freely and collide elastically [2]. The cavity Q is separated from from the complement of the cavity Q^c by a boundary δQ. Potential in the cavity is $V = 0$ and at the boundary the potential approaches infinity i.e., $V \to \infty$. The particles bounce from the boundary with the same angle as the incoming angle ϕ and with the same absolute momentum $|\boldsymbol{p}|$ as before the collision as shown in Fig. 2.1.

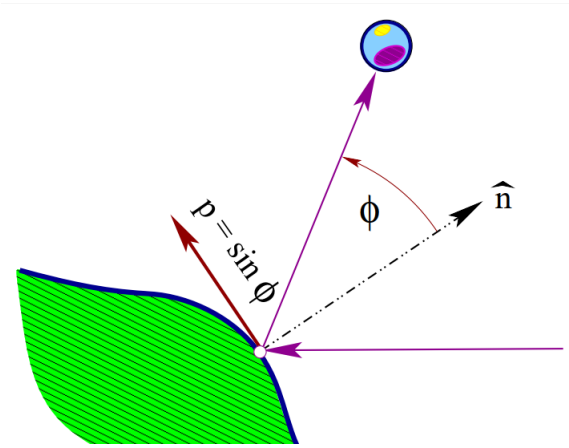

Figure 2.1. *Example of a classical particle colliding with the billiard boundary δQ (modified from Ref. [2])*

The incoming angle is defined with respect to the surface normal $\hat{n}$ which is a vector that points away from the surface in an angle of $\pi/2$ radians. There are two directions in which the surface normal can point, but it is defined to point inside to the cavity.

Chaos can be described as an undeterministic nature of the time evolution of a deterministic system if its initial condition is not precisely defined [8, 9]. In other words, in a chaotic system a slight change of the initial conditions affects the resulting state considerably. Examples of chaotic billiard systems are shown in Figs. 2.2b and 2.2c.

The opposite of a chaotic system is called an integrable system where the motion of particles is predictable. An example of a integrable system is a square billiards demonstrated in Fig. 2.2a.

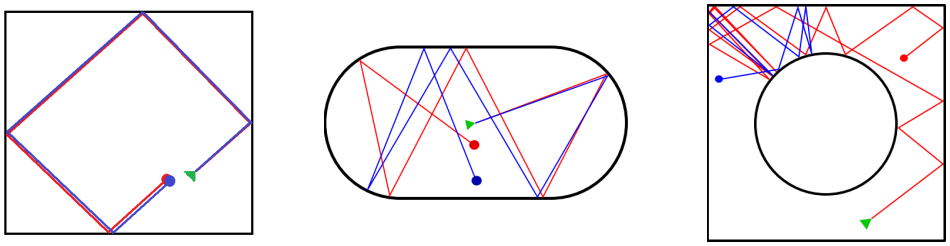

(a) ***(b)*** ***(c)***

Figure 2.2. *Two trajectories with slightly different initial conditions in (a) a rectangular billiards, (b) stadium billiards and (c) Sinai billiards.*

In integrable systems the angle after collision ϕ has fewer possible values with which the particles can collide from the boundary and the angles often follow a certain sequence within a specific trajectory. Thus, in an integrable cavity the trajectories are more predictable. In contrast, in a chaotic cavity the trajectory is much more erratic, since it will eventually collide with every possible angle against the boundary of the cavity. Therefore, the trajectory is more difficult to predict in a chaotic cavity.

For example, a slight deviation in the initial conditions of a particle colliding both in the half-circles and in the straight boundaries of the stadium changes the outgoing trajectory

of the particle much more than in a rectangle. Thus, by definition, the stadium is more chaotic than a rectangle [2]. Since a rectangle is less chaotic there are more repeating trajectories, i.e., the particle ends after a finite time in the same position with same direction of motion. If the cavities had a small opening on the side, a particle would more likely hit the hole in a chaotic system than in an integrable one [1].

2.3 Quantum billiards

In contrast to classical billiards, quantum billiards cannot be formulated in terms of elastic collisions with the boundary. Instead, quantum billiards are governed by the Schrödinger equations with Dirichlet boundary conditions [10, 11].

Quantum billiards can also be evaluated by examining the evolution of a quantum mechanical wave packet inside the cavity [12]. This is not as straightforward as in classical billiards since the wave packet spreads out to the whole system due to dispersion. Some high-probability areas may eventually emerge during the time evolution [10]. These areas are called quantum scars.

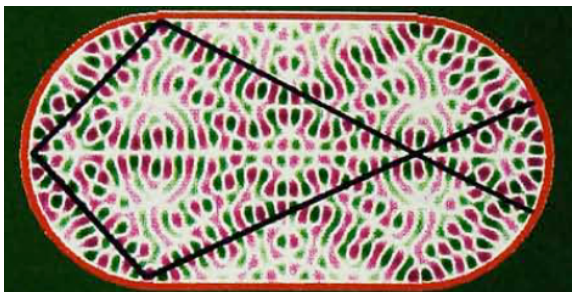

Figure 2.3. *Example of scars in a quantum mechanical system (taken from Ref. [10])*

Scars resemble periodic classical trajectories in the system. These states can be calculated using a semiclassical approach. Figure 2.3 shows scars around a periodic classical trajectory drawn with a black line.

It has been shown that billiard systems that are classically chaotic do not necessarily exhibit chaos when examined as a quantum mechanical system [13]. Therefore, the escape rate as described in Sec. 2.2 cannot be formulated similarly for the quantum mechanical case.

Instead, a quantum mechanical escape rate can be formulated by evaluating how much of a wave packet or the corresponding probability density spreads out of the cavity. To assess the position of a quantum mechanical particle in a connected cavity system, one only needs to compare the integrated probability densities between the cavities.

3 COMPUTATIONAL METHODS

3.1 Simulation

The wave packet that we initialize in the cavity needs to have a boundary in which it is zero within the specified cavity. Thus, we define it as a modified version of a Gaussian wave packet:

$$\psi(r_0, 0) = \begin{cases} \exp\left(\frac{-\log 2}{1-\frac{(r-r_0)^2}{4\sigma^2}} \cdot \frac{(r-r_0)^2}{2\sigma}\right), |r - r_0| < 2\sigma \\ 0 \qquad\qquad\qquad\qquad , |r - r_0| \geq 2\sigma \end{cases} \tag{3.1}$$

Here r is the position, r_0 is the initial position and σ is the full width at half maximum. The wave packet also needs the initial velocity. It is defined by multiplying initial wave packet by

$$e^{-i \cdot p \cos\theta \cdot x - i \cdot p \sin\theta \cdot y}, \tag{3.2}$$

where θ is the angular direction with respect to horizontal axis and p is the momentum of the wave packet.

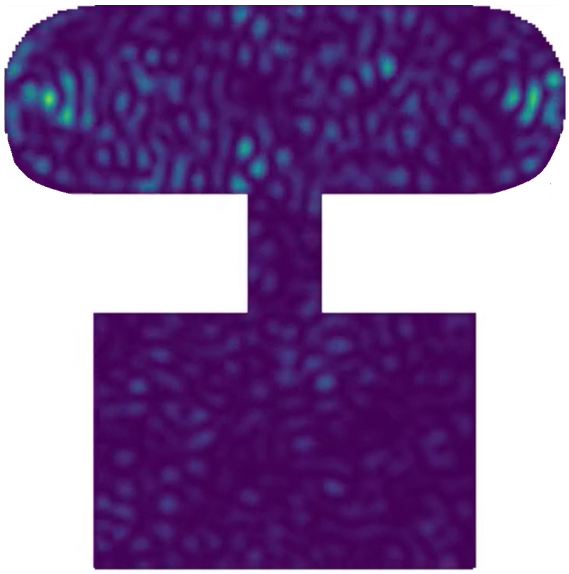

Figure 3.1. *Simulation box with a propagated wave function inside*

We define a connected two-cavity system with Dirichlet boundary conditions as shown in Fig 3.1. On a Dirichlet boundary the wave function has a zero value [14]. The cavities were chosen to have a shape of a rectangle and a stadium as discussed in Sec. 2.2. The areas of the cavities are equal.

A wave packet is initialized in one of the cavities, and the Octopus simulation package is used to compute its time evolution by numerically solving the time-dependent Schrödinger equation [15, 16]. The grid spacing in the system is defined to be $dx = dy = \frac{1}{|\boldsymbol{p}|+3\cdot\sigma}$. The time-step of the simulation is one-tenth of the grid size. The grid size was then optimized to be small enough to maintain accurate simulation results but sufficiently large to allow the minimal computing time.

3.2 Observables

3.2.1 Probability

A quantum mechanical particle is described by a wave function ψ. The square of the norm of the wave function describes the probability density $\rho = |\psi|^2$. The time-dependent probability $P_\Omega(t)$ of finding the particle in the cavity Ω (rectangle or stadium) is thus given by

$$P_\Omega(t) = \int_\Omega |\psi(x, y, t)|^2 \cdot \mathrm{d}\boldsymbol{r}, \tag{3.3}$$

where x and y are the spatial coordinates and t is the time. We can approximate $P_\Omega(t)$ by

$$P_\Omega(t) \approx \sum_{(x,y)\in\Omega} \rho(x, y, t) \cdot \Delta x \Delta y, \tag{3.4}$$

where Δx and Δy are the grid spacings in respective directions. At each time step the total probability in the whole system covering the cavities and the tunnel should be exactly one. This is used to verify that the calculation is correct.

3.2.2 Autocorrelation

Autocorrelation $|A(t)|^2$ measures how much the state at time t resembles the original state [17]. It is calculated by comparing the state of the system at time t to the original state at time $t = 0$. A high value for autocorrelation means that the system at time t resembles the original state of the system. The autocorrelation can be calculated from

$$|A(t)|^2 = \left| \int \psi^*(\boldsymbol{r}, 0) \cdot \psi(\boldsymbol{r}, t) \cdot \mathrm{d}\boldsymbol{r} \right|^2, \tag{3.5}$$

where ψ^* is the complex conjugate of ψ. It can be approximated as

$$|A(t)|^2 = \left| \sum_{x,y} \psi^*(x,y,0) \cdot \psi(x,y,t) \cdot \Delta x \Delta y \right|^2 . \tag{3.6}$$

Autocorrelation is calculated for the whole system and not for specific cavity in the system. Note that calculation of the autocorrelation function needs the wave function ψ and not the probability density ρ.

3.2.3 Localization

We also want to know to which extent the wave packet is spread out in the system. This can be assessed with locality functions such a thes inverse participation ratio (IPR) and information entropy (IE) [18, 19, 20]. These localization functions are defined as

$$L^{\mathsf{IPR}}(t) = \left[\int |\psi(\boldsymbol{r},t)|^4 \cdot \mathrm{d}\boldsymbol{r} \right]^{-1} \text{ and} \tag{3.7a}$$

$$L^{\mathsf{IE}}(t) = e^{-\int |\psi(\boldsymbol{r},t)|^2 \cdot \log(|\psi(\boldsymbol{r},t)|^2) \cdot \mathrm{d}\boldsymbol{r}}. \tag{3.7b}$$

A higher value of the localization function corresponds to a widely spread-out wave packet. Likewise, a low value corresponds to a localized wave packet. For computational purposes the localization functions can be approximated as

$$L^{\mathsf{IPR}}(t) \approx \left[\sum_{x,y} |\rho(x,y,t)|^2 \cdot \Delta x \Delta y \right]^{-1} \text{ and} \tag{3.8a}$$

$$L^{\mathsf{IE}}(t) \approx e^{-\sum_{x,y} \rho(x,y,t) \cdot \log(\rho(x,y,t)) \cdot \Delta x \Delta y}. \tag{3.8b}$$

Even though IPR and IE are noticeably different, they measure the same phenomenon and should thus behave similarly. This fact is used as reassurance of the calculations and conclusions.

3.2.4 Convergence with respect to grid size

An appropriate grid size can be determined by several simulations where the parameters of the simulation are kept the same except that the grid spacing is changed. The probabilities obtained for each grid size are then compared to the probabilities P_Ω with the densest grid. At each time step the average and maximum absolute difference is compared.

4 RESULTS

In this chapter we examine the results of the simulation of a quantum mechanical wave packet in a double cavity as described in Sec. 3.1. The observables were calculated as described in Sec. 3.2. The results are then discussed with respect to Maxwell's demon, and whether evidence of it can be found in the double cavity system.

4.1 Grid size

As discussed in Sec. 3.2.4 the correct grid size is important for an accurate yet fast simulation. Let us compare the results of several simulations with the same initial conditions but with different grid sizes.

Simulation number	Grid size	Spacing (a.u.)
1.	20 x 30	0.1
2.	40 x 60	0.05
3.	80 x 120	0.025
4.	100 x 150	0.02
5.	200 x 300	0.01
6.	400 x 600	0.005

Table 4.1. *Grid sizes and spacing's used in the simulations.*

The different grid sizes used in the simulations are presented in table 4.1. The cavity has a size of 2 a.u. by 3 a.u..

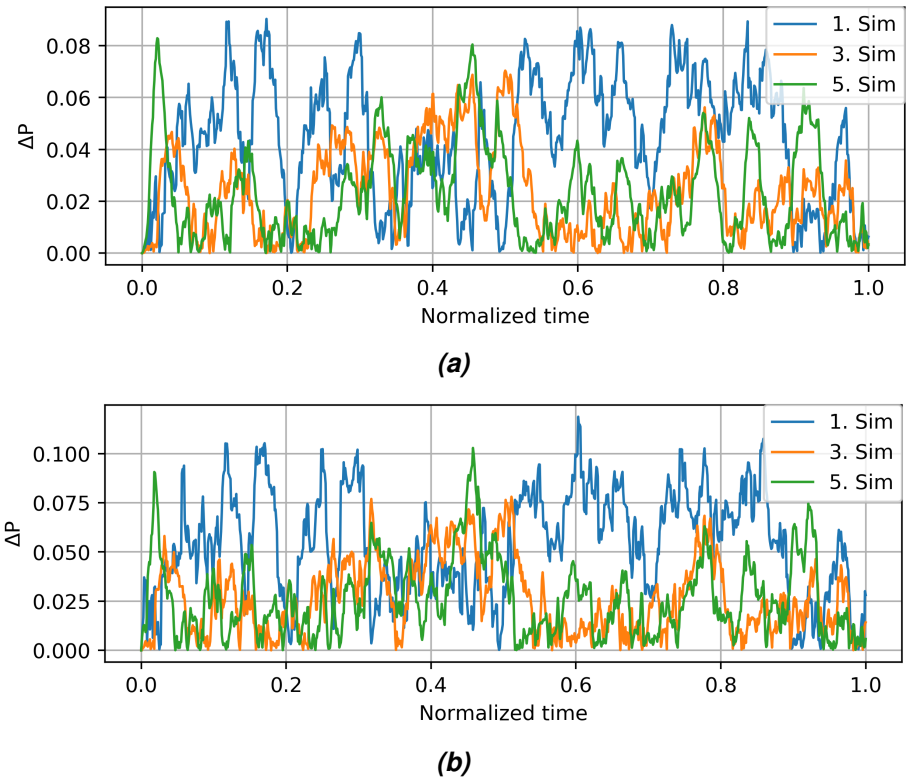

Figure 4.1. *Absolute differences of the cavity probabilities $P_\Omega(t)$ for the box (a) and the the stadium (b) with respect to the simulation with the densest grid.*

The absolute differences in the total probability as shown in Eq. (3.4) at each time step with respect to grid size are presented in Figs. 4.1a and 4.1b. Based on the values in Figs. 4.1a and 4.1b maximum and average differences were calculated and they are presented in Figs. 4.2a and 4.2b respectively.

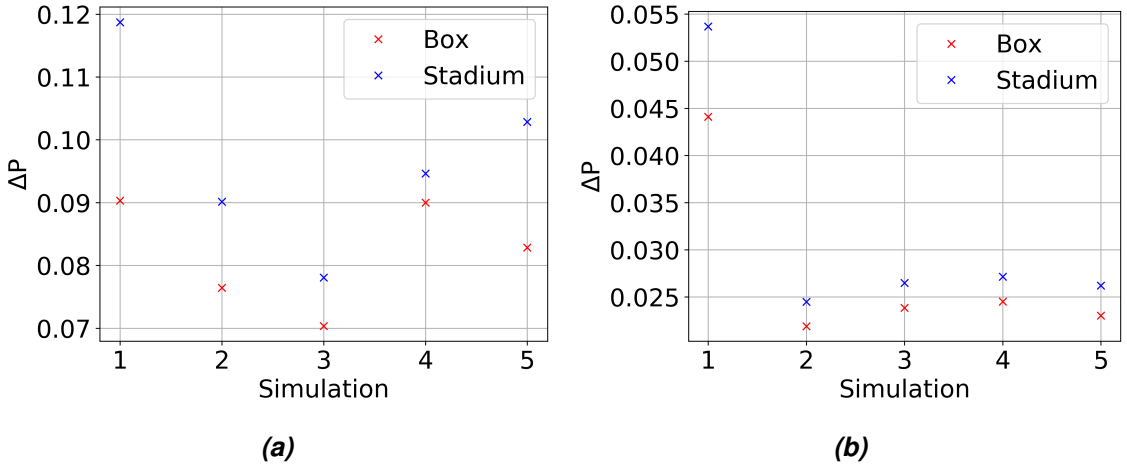

Figure 4.2. *(a) maximum differences and (b) average differences of probabilities with respect to the densest grid of $dx = 0.005$ a.u..*

Based on these results a grid size of 200 by 300 or the fifth simulation of the convergence test was chosen, since for the next grid size of 400 by 600 the test simulation took a little over two hours, which is too long to do several consecutive simulations.

4.2 Comparison between integrable and chaotic cavities

In this section we examine the evolution of the quantum mechanical particle inside the double cavity system in more detail. More precisely, the differences between the evolution with respect to starting from either of the two cavities is studied. Based on the differences we can then comment on the existence of Maxwell's demon in the quantum mechanical double cavity system.

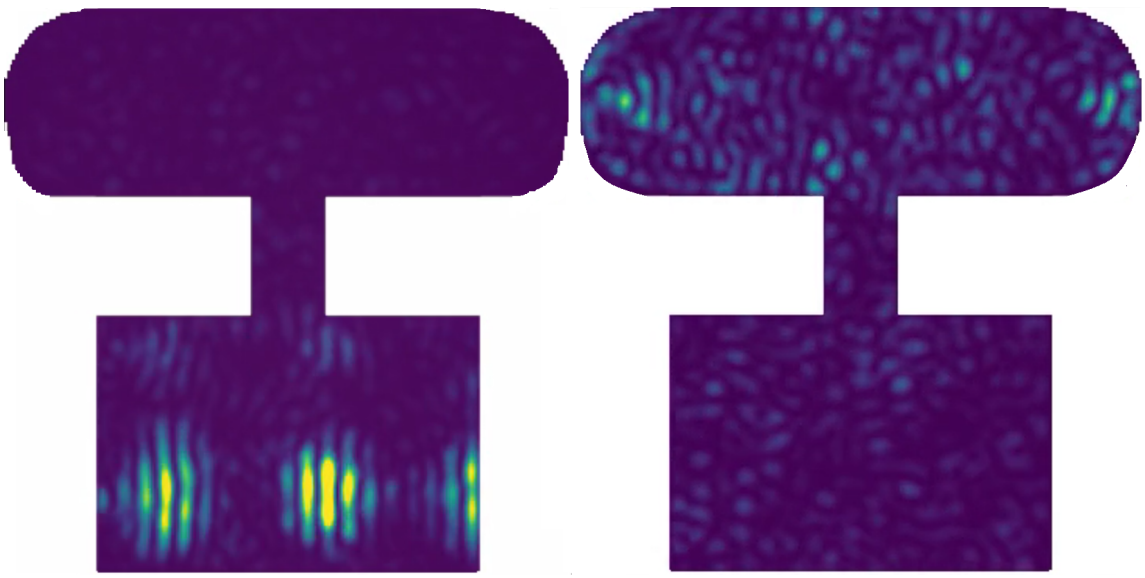

(a) ***(b)***

Figure 4.3. *A snapshot of the probability density when initializing the wave packet in (a) the rectangle and (b) the stadium*

As an illustration of typical quantum dynamics in the system, we show examples of propagated wave packets in Fig. 4.3a. We see pronounced localization of the wave packet when the wave packet is initialized in rectangle. Similar effects cannot be seen in Fig. 4.3b when the wave packet initialized in stadium. In the following we focus on the probabilities, autocorrelation and localization of the wave packet.

4.2.1 Probability

If we start at either cavity and measure the system at certain intervals, based on classical results discussed above, we may expect that we are more likely to find the quantum particle in the non-chaotic rectangular cavity.

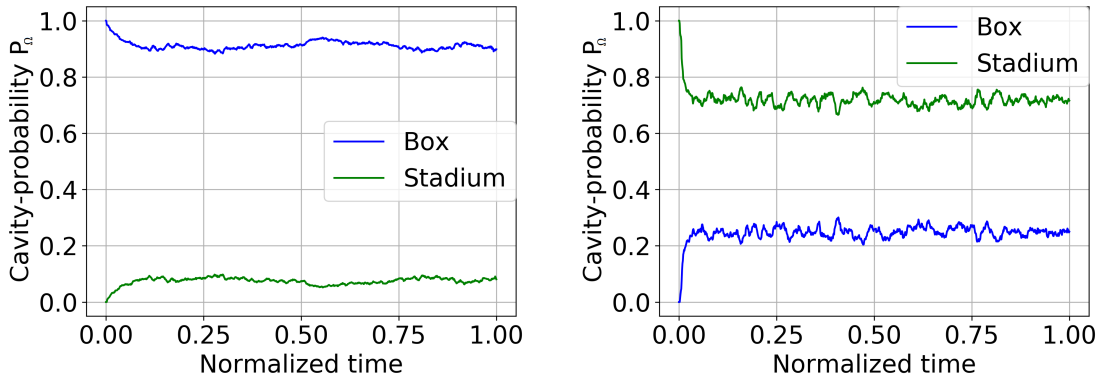

Figure 4.4. *Cavity-probabilities $P_\Omega(t)$ when wave packet starts in (a) the box or (b) the stadium.*

The probabilites calculated with Eq. (3.4) are presented in Figs. 4.4a and 4.4b for starting positions in the box or stadium, respectively. In these figures the total probability is not necessarily equal to one as some part of the wave packet is always in the connecting tunnel after the initial state. The probability in the tunnel is left out since it is negligible and does not affect the main conclusions.

The cavity-probability decreases in the cavity where the packet is initialized. It decreases more when the wave packet is initialized in the stadium rather than vice versa. In other words, the wave packet leaks out from the stadium more than from the rectangle.

4.2.2 Autocorrelation

In Figs. 4.5a and 4.5b we show the calculated autocorrelations according to Eq. (3.6).

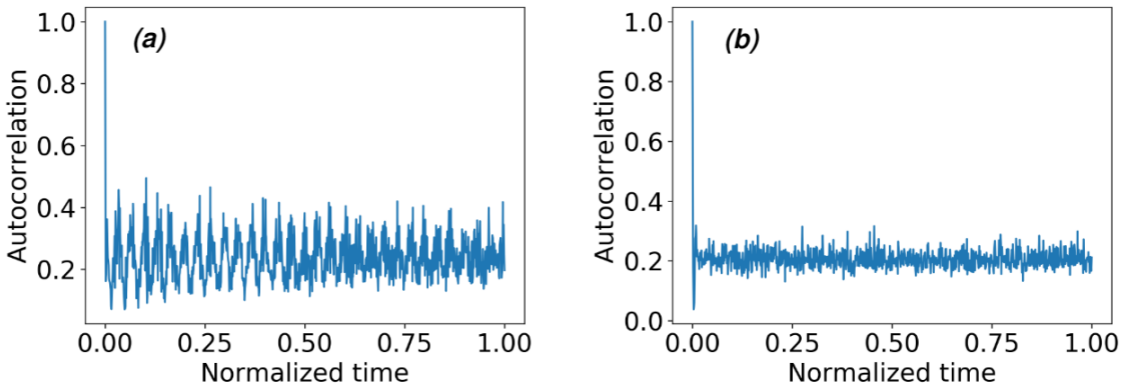

Figure 4.5. *Autocorrelation evolution of a dual-cavity system when the wave packet starts in (a) the box or in (b) the stadium.*

We find that the system is more likely to resemble a bit of itself when starting inside the rectangle compared to starting inside the stadium. It will also at certain times resemble less the original system. This indicates that the wave packet clumps together inside the cavity and is less spread out, since a large portion of the wave packet is where it was

initially.

4.2.3 Localization

In Figs. 4.6a and 4.6b we show the IE localization of the system as a function of time according to Eq. (3.8b). In Fig. 4.6a the wave packet starts in the box and in Fig. 4.6b the wave packet starts in the stadium.

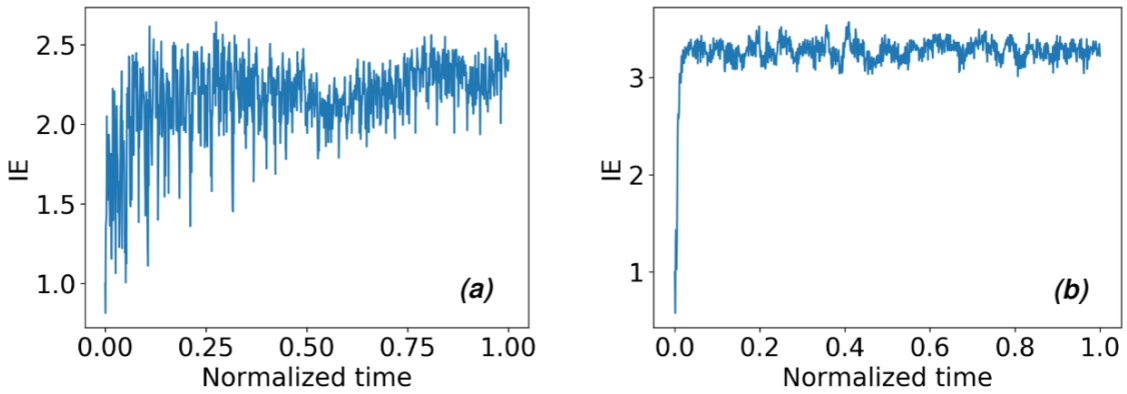

Figure 4.6. *Information entropy localization evolution of dual-cavity system when the wave packet starts in (a) the rectangle and (b) in the stadium.*

As mentioned in Sec. 4.2.2, when starting inside the rectangle the wave packet seems to remain more localized during the evolution. This is confirmed with localization calculations. We see that the maximum localization is lower when starting from the rectangular cavity. The localization calculation values also oscillate much more for the rectangle and even localizes a little at times. For the stadium however once spread out the value of localization keeps relatively constant.

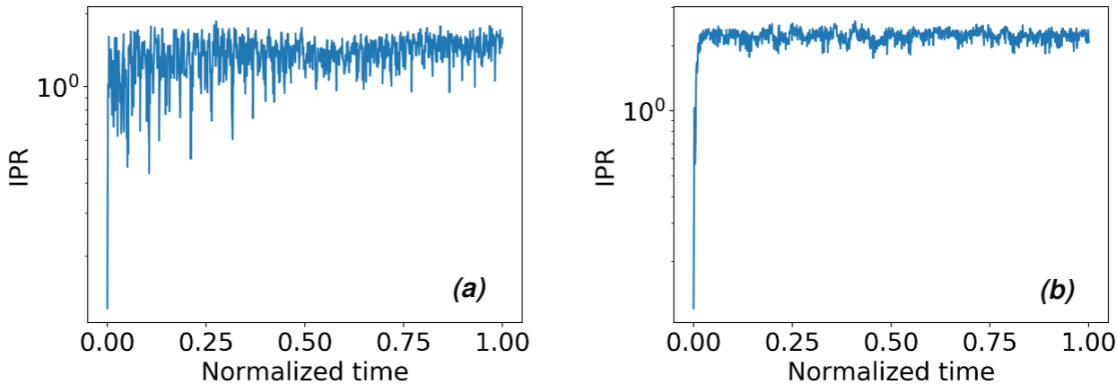

Figure 4.7. *Inverse participation ratio localization evolution of dual-cavity system when the wave packet starts in (a) the rectangle and (b) the stadium.*

The IPR localization calculated with Eq. (3.8a) is presented in Figs. 4.7a and 4.7b. The results are qualitatively similar to those obtained for the IE localization. This is plausible in view of the similar definitions of the IE and IPR localization.

4.3 On the existence of quantum Maxwell's demon

We see in Sec. 4.2.1 that when initializing the wave packet inside the stadium the wave packet leaks in to the other cavity much more than vice versa. From the results in Sec. 4.2.2 we see that the wave packet resembles the original tightly packed state more when initialized in the rectangular cavity. From the localization calculations in Sec. 4.2.3 we can conclude that the wave packet groups into clumps when initialized in the rectangle and that initializing in the stadium the wave spreads out more.

In the animation (see Fig. 4.3a for a snapshot) we find that, when starting in the integrable cavity, a ball bouncing from side to side emerge every now and then. In the chaotic cavity the wave packet spreads out to the whole two-cavity system without grouping together afterwards.

Combining the results above, we conclude that the wave packet has a clear tendency to favor the integrable cavity, thus giving rise to a quantum mechanical Maxwell's demon. This result is expected since for the classical counterpart the integrable cavity is less ergodic than the chaotic cavity in other words a classical particle is more likely to visit every point in the chaotic cavity.

If the system was measured periodically the wave packet will appear in the integrable cavity more often than not. Since the wave packet has always some ripples in the cavity where it wasn't initialized in, and when initialized in the chaotic cavity it has more ripples in the other cavity than when initialized in the integrable one. This suggests it will more likely be measured to be inside the other cavity when initialized in the chaotic cavity than vice versa. Any new measurement can be considered a start of a new sequence of measurements, so the quantum particle can be measured to be in either cavity at any time. However, most of the measurements will find it to be inside the integrable cavity, thus showing that Maxwell's demon appears in a quantum mechanical system.

The results considered here are based on a small amount of simulations and initial conditions. This means the results are approximate but reliable. However, more accurate treatment would need more simulations with varying initial conditions.

5 SUMMARY

In this thesis we have investigated the existence of Maxwell's demon in a quantum mechanical double-cavity system. Maxwell's demon in the case of a quantum mechanical system appears as a higher probability over time of measuring a particle in one cavity rather than the other.

The studied system was constructed of a chaotic stadium-shaped cavity, a non-chaotic rectangular cavity, and a tunnel connecting the two. Inside the cavity a quantum mechanical wave packet was released to propagate.

The probability of the quantum mechanical particle to be found in a certain cavity, autocorrelation and localization were calculated as a function of time. Autocorrelation describes how the system resembles the original state, and the localization describes the spreading of the wave packet in the cavity system.

When the wave packet starts its propagation inside the chaotic stadium-shaped cavity, it spreads out to the whole double-cavity system almost evenly. In contrast, when the wave packet starts inside the non-chaotic rectangular cavity, it bounces inside the rectangle as a compact ball with minimal spreading to the rest of the double cavity.

We see that in the double-cavity system the wave packet does have a higher probability to end up and stay in the integrable rectangular cavity. In other words, we do see a Maxwell's demon in the quantum mechanical system.

A more thorough study, including a quantitative comparison between a classical and quantum simulation is needed to find out and to characterize the precise quantum fingerprints of Maxwell's demon. This is the topic of a future study.

REFERENCES

[1] Blundell, S. and Blundell, K., *Concepts in Thermal Physics*, 2nd edition. Department of Physics, University of Oxford, UK, (2010).

[2] Cvitanović, P., Artuso, R., Mainieri, R., Tanner, G. and Vattay, G., *Chaos: Classical and Quantum*. ChaosBook.org (Niels Bohr Institute, Copenhagen), (2016).

[3] Haake, F., *Quantum Signatures of Chaos*, 3rd edition. Springer-Verlag Berlin Heidelberg, (2010).

[4] Knott, C., *Life and Scientific Work of Peter Guthrie Tait*. Cambridge University Press, (1911).

[5] Michael, M. and Colm, O., *Understanding Physics*, 2nd edition. John Wiley Sons, (2011).

[6] Rex, A., Maxwell's demon—a historical review, *Entropy*, vol. 57, (1998).

[7] Shannon, C., A mathematical theory of communication, *The Bell System Technical Journal*, vol. 27, 379–423, (1948).

[8] Lorenz, E., Deterministic nonperiodic flow, *Journal of the Atmospheric Sciences*, vol. 20, 130–141, (1963).

[9] Danforth, C. (2013). Mathematics of planet earth, Chaos in an atmosphere hanging on a wall, [Online]. Available: `http://mpe.dimacs.rutgers.edu/2013/03/17/chaos-in-an-atmosphere-hanging-on-a-wall/` (visited on 03/18/2020).

[10] Heller, E. J. and Tomsovic, S., Postmodern quantum mechanics, *Physics Today*, vol. 46, 38–46, (1993).

[11] Griffiths, D., *Introduction to Quantum Mechanics*, 2nd edition. Pearson Education Inc., (2005).

[12] Baowen Li, M. R. and Hu, B., Relevance of chaos in numerical solutions of quantum billiards, *Physical Review E*, vol. 19, 240, (2017).

[13] Antonsen Jr, T. M., Ott, E., Chen, Q. and Oerter, R. N., Statistics of wave-function scars, *Physics Review E*, vol. 51, 111–121, (1995).

[14] A. Cheng, D. C., Heritage and early history of the boundary element method, *Engineering Analysis with Boundary Element*, vol. 29, (2005).

[15] Tancogne-Dejean, N. et al., Octopus, a computational framework for exploring light-driven phenomena and quantum dynamics in extended and finite systems, *The Journal of Chemical Physics*, vol. 152, (2020).

[16] Solanpää, J., Optimization of ultrafast strong-field phenomena, *Tampere University Dissertations*, vol. 82, (2019).

[17] Gubner, J., *Probability and Random Processes for Electrical and Computer Engineering*. Cambridge University Press, (2006).

[18] Wegner, F., Inverse participation ratio in 2+ dimensions, *Zeitschrift für Physik B Condensed Matter*, vol. 36, 209–214, (1980).

[19] Kramer, B. and MacKinnon, A., Localization: Theory and experiment, *Reports on Progress in Physics*, vol. 56, 1469–1564, (1993).

[20] Gong, L. et al., The relations among shannon information entropy, quantum discord, concurrence and localization properties of one-dimensional single-electron wave functions, *Nonlinearity*, vol. 4, 59–84, (1991).